$F(\alpha)$ Spectrum of Pruned Baker's Map

Paul Jenkins [1], Mark V. Daly [1], and Daniel M. Heffernan [1,2,3]

[1] School of Physical Sciences, Dublin City University, Glasnevin, Dublin 9, Ireland
[2] School of Theoretical Physics, Dublin Institute of Advanced Studies, Dublin 4, Ireland
[3] Department of Mathematical Physics, St. Patrick's College, Maynooth, C. Kildare, Ireland

Z. Naturforsch. **48a**, 1166–1172 (1993); received September 30, 1992

We study in detail the evolution of fractal structure within a two dimensional hyperbolic baker's map with a complete set of unstable orbits. The evolution of fractal structure within the phase space of the map is related to changes in an associated Cantor set, and this evolution is studied via their corresponding $f(\alpha)$ spectra. Numerical calculations of unstable periodic orbits for a related baker's map, with an incomplete set of unstable orbits, is investigated and directly related to, and characterized by, a pruned Cantor set. The effect of the pruning on the associated $f(\alpha)$ spectrum of the baker's map is analyzed.

Key words: Chaos; Baker's map; Cantor set; Generalized dimension; $f(\alpha)$ spectrum.

1. Introduction

One of the simplest and most studied dynamical system is the baker's map [1]. The baker's map is fundamental to statistical physics [2] and both classical and quantum chaos [3]. One can completely characterize chaos in the standard baker's map. It has a complete binary tree (orbit structure), and this enables one to treat the problem analytically. However in dynamical systems studied to date if the binary tree is incomplete, the characterization of chaos, in particular the effect on the generalized dimensional spectrum and its $f(\alpha)$ spectrum, is not yet fully understood [4, 5]. In this paper we analyze the effect of an incomplete orbit structure on the $f(\alpha)$ spectrum of the baker's map. The paper is organized as follows.

In Sect. 2 we review the theory of Cantor sets which is pertinent to the characterization of chaos in baker's map. In Sect. 3 the evolution of structure in the baker's map is characterized using $f(\alpha)$ and $g(\lambda)$ spectral techniques. In Sect. 4 the correspondence between a baker's map with an incomplete set of periodic orbits and a pruned Cantor set is examined. The effect of the incomplete set of orbits on the $f(\alpha)$ spectrum of the map is analyzed. Numerical methods are used both to extract these periodic orbits and to compute the $f(\alpha)$ spectrum.

Reprint requests to Professor D. M. Heffernan, Department of Mathematical Physics, St. Patrick's College, Maynooth, Co. Kildare, Ireland.

2. Two Scale Cantor Sets

Baker's maps, for parameter ranges where they are chaotic, have a strange attractor with a Cantor set, underlining their phase space structure. In this section we review that part of the theory of Cantor sets which is pertinent to our analysis, namely, two scale recursive sets. A two scale Cantor set is generated by the following process. Start with an original region that has measure one and size one. Divide this region into two pieces of length l_1 and l_2 with probabilities P_1 and P_2, respectively, such that $P_1 + P_2 = 1$ and $l_1 + l_2 \leq 1$. The partition function is given by

$$\Gamma(\tau, q) = \left[\frac{P_1^q}{l_1^\tau} + \frac{P_2^q}{l_2^\tau}\right]^n = 1\,. \tag{1}$$

As $n \to \infty$, Γ does not depend on n. This partition function is of the order of unity only when $\tau(q) = (q-1)D_q$ [6]. A binomial expansion of (1) gives

$$\Gamma(q, \tau) = \sum_{m=0}^{\infty} \binom{n}{m} P_1^{mq}\, P_2^{(n-m)q} (l_1^m\, l_2^{(n-m)})^{-\tau(q)} = 1\,. \tag{2}$$

Using the analytic methods of Halsey et al., analytic expressions for the $f(\alpha)$ spectrum can be obtained [6]:

$$f = \frac{(n/m-1)\ln(n/m-1) - (n/m)\ln(n/m)}{\ln(l_1) - (n/m-1)\ln(l_2)} \tag{3}$$

with the exponent determining the singularity in the measure, α, given by

$$\alpha = \frac{\ln(P_1) + (n/m-1)\ln(P_2)}{\ln(l_1) - (n/m-1)\ln(l_2)}\,. \tag{4}$$

0932-0784 / 93 / 1200-1166 $ 01.30/0. – Please order a reprint rather than making your own copy.

Thus, for any chosen q, the measure scales as $\alpha(q)$ on a set of segments which converge to a set of dimension $f(q)$. In Fig. 1 the $f(\alpha)$ spectrum for the two scale Cantor set is shown, with probabilities $P_1 = 0.6$ and $P_2 = 0.4$, rescaling length $l_2 = 0.1$, and for three different values of length scale l_1, namely 0.1, 0.3 and 0.7. As q is varied, different regions of the set determine D_q. The extreme α values are

$$D_{-\infty} = \alpha_{\max} = \ln P_2/\ln l_2$$

and (5)

$$D_{\infty} = \alpha_{\min} = \ln P_1/\ln l_1 .$$

For $q=0$ we simply obtain $f=D_0$, where D_0 is the Hausdorff dimension of the set. From (1) the maximum D_0 is defined by the transcendental equation

$$l_1^{D_0} + l_2^{D_0} = 1 . \tag{6}$$

With increasing l_1, D_0 tends to its maximum value of 1. These Cantor sets are multifractal and underlie the structure of many strange attractors that occur in physics [6].

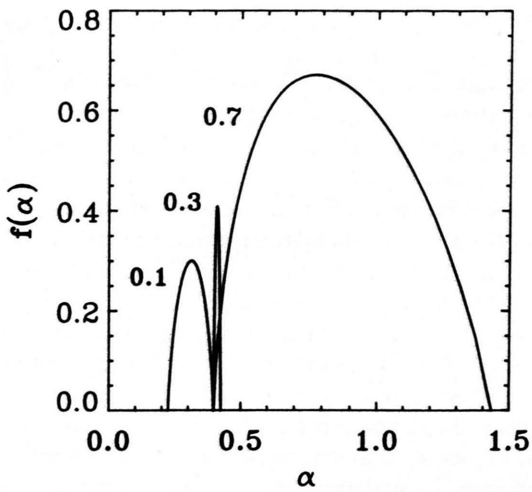

Fig. 1. A plot of $f(\alpha)$ vs. α for the two scale Cantor set, with probabilities $P_1=0.6$ and $P_2=0.4$, rescaling length $l_2=0.1$ for three different values of length scale l_1, namely 0.1, 0.3, and 0.7.

3. The Baker's Map

The generalized baker's map is defined [7, 8] by the recursion relations on the unit square

$$\begin{pmatrix} X_{i+1} \\ Y_{i+1} \end{pmatrix} = \begin{cases} \begin{pmatrix} R_1 X_i \\ Y_i/S \end{pmatrix} & 0 \le Y \le S \\ \begin{pmatrix} 1/2 + R_2 X_i \\ (Y_i - S)/(1-S) \end{pmatrix} & S < Y \le 1 \end{cases} \tag{7}$$

with $R_1, R_2 < 1/2$, $S < 1$. This is a hyperbolic system with a uniform probability density along the unstable manifold. For hyperbolic maps, stable and unstable manifolds are defined everywhere. The attractor lies along the unstable manifold which is in the Y direction with the Cantor set in the X direction. This manifold, which originates from the periodic orbits, consists of an infinite number of line segments.

Using symbolic dynamics with the partition $\chi(X, Y) = 1$ for $Y > S$ and $\chi(X, Y) = 0$ for $Y < S$, we find that every sequence of 1's and 0's is allowed and that there are 2^n orbits belonging to an unstable orbit of period n [9]. The eigenvalues of the n-cycle depend only on the number of 1's and 0's in the sequence. Denoting the number of 0's by m, we find that the Lyapunov scaling factors at the n-th iteration are given by [9–11]

$$\varepsilon_1^{(n)} = S^{-m}(1-S)^{-(n-m)}, \quad \varepsilon_2^{(n)} = R_1^m R_2^{(n-m)} . \tag{8}$$

For hyperbolic attractors, the partition function is related to the stability of the unstable orbits by [11]

$$\Gamma(q, D) = \sum \varepsilon_1^{-q} \varepsilon_2^{-\tau(q)} , \tag{9}$$

where the sum is over all allowed unstable orbits of period n. To account for the dimension along the unstable manifold, $\tau(q)$ is defined as $\tau(q) = (D_q - 1)(q-1)$. Inserting (8) into (9), we obtain

$$\Gamma(q, D) = \sum_{m=0}^{n} N_{nm} S^{mq}(1-S)^{(n-m)q}(R_1^m R_2^{(n-m)})^{-\tau(q)} , \tag{10}$$

where N_{nm} is the number of fixed points of the n times iterated map which belong to a periodic orbit with m 0's in its sequence. N_{nm} is just the number of ways of arranging m zeros and $n-m$ ones,

$$N_{nm} = \binom{n}{m} . \tag{11}$$

Apart from the power $(D_q - 1)$, (10) is equivalent to the partition function of (2) which was obtained for the two scale Cantor set. The parameters S, $(1-S)$, R_1 and R_2 are related to P_1, P_2, l_1 and l_2, respectively, of the two scale Cantor set, namely, $S=P_1$, $(1-S)=P_2$, $R_1 = l_1$ and $R_2 = l_2$ [9]. Thus for this baker's map the

Cantor structure of the attractor can be explicitly obtained.

For parameters $S = 1/2$ and $R_1 = R_2 = R$, the baker's map is equivalent to the uniform Cantor set with a point $f(\alpha)$ spectrum. The evolution of structure within the attractor of this map as the parameter R is varied is shown in Figs. 2a–d for the parameter values $R = 0.1, 0.3, 0.4$ and 0.5, respectively. The corresponding dimensions D_q are 1.3, 1.58, 1.75 and 2.0. The first three are examples of strange attractors and are self similar under all scales of magnification. As the parameter R is increased, the unstable orbits redistribute causing changes in the structure of the attractor. Since the dimension D_q in the Y direction is constant, the increase in dimension and the corresponding change in structure are directly related to the changes in the underlieing Cantor set.

The generalized entropy, K_q, can be calculated from the equation [12],

$$\sum_{m=0}^{n} \binom{n}{m} S^{mq}(1-S)^{(n-m)q} = \exp(-n\,\vartheta(q))\,, \quad (12)$$

where $\vartheta(q) = (q-1)K_q = \lambda q - g(\lambda)$ and $g(\lambda)$ is the fluctuation spectrum around the K-entropy [1]. In the limit $n \to \infty$ the largest term in the sum of the right hand side of (12) should dominate. To find this term, we note that the maximum occurs when

$$\frac{\delta}{\delta m} \ln \binom{n}{m} S^{mq}(1-S)^{(n-m)q} = 0\,. \quad (13)$$

Using Stirling's approximation, we find,

$$q = \frac{\ln(n/m - 1)}{\ln(1-S) - \ln(S)}\,. \quad (14)$$

The fluctuation spectrum is determined by

$$\binom{n}{m} = \exp(n\, g(\lambda)) \quad (15)$$

which, on applying Stirling's approximation, yields

$$g = \ln(n/m) - (1 - m/n)\ln(n/m - 1)\,. \quad (16)$$

The exponent determining the singularity in the measure, λ, is determined by .

$$S^{mq}(1-S)^{(n-m)q} = \exp(-n\,\lambda q) \quad (17)$$

or

$$\lambda = \frac{m\ln(S) + (n-m)\ln(1-S)}{-n}\,. \quad (18)$$

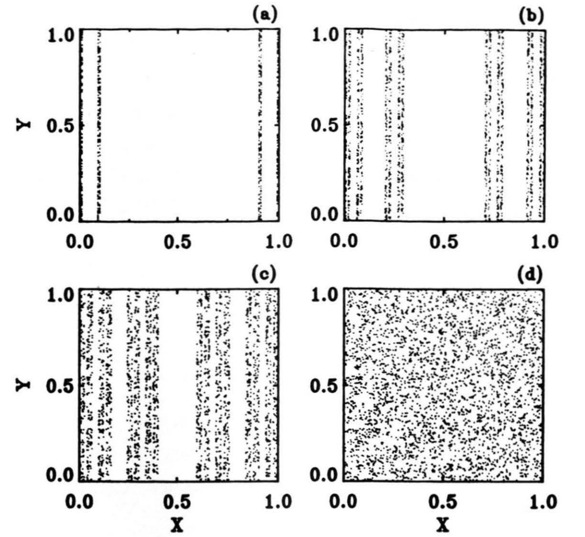

Fig. 2. The evolution of structure within the attractor of the baker's map as the parameter R is varied. The figures shown are for $S=1/2$ and four values of the parameter R, namely, (a) $R=0.1$, (b) $R=0.3$, (c) $R=0.4$ and (d) $R=0.5$. The structure of these attractors is related to the middle third Cantor set.

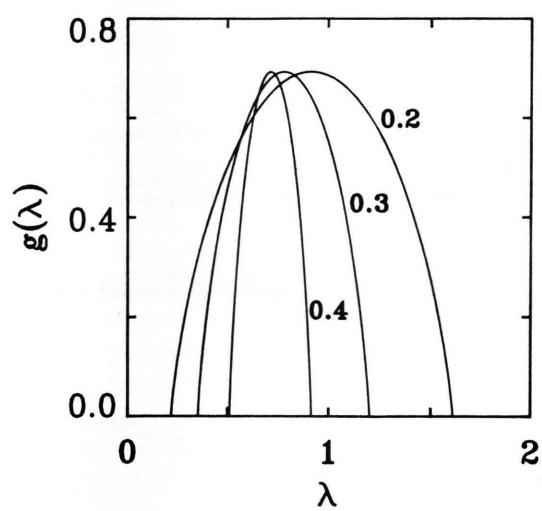

Fig. 3. The generalized spectrum $g(\lambda)$ versus λ for three different values of S, namely $S=0.2$, 0.3, and 0.4. The range of λ extends for fixed S, from $-\ln(1-S)$ to $-\ln(S)$.

Thus, for any chosen q, the measure scales as $\lambda(q)$ on a set of segments which converge to a set of entropy $g(q)$. As q is varied, different regions of the set determine K_q. In Fig. 3 we show the $g(\lambda)$ spectrum of the baker's map for the parameters $S=0.2$, 0.3 and 0.4.

4. Pruned Baker's Map

Consider the baker's map in the form [13]

$$\begin{pmatrix} X_{i+1} \\ Y_{i+1} \end{pmatrix} = \begin{cases} \begin{pmatrix} R_1 X_i \\ T\, Y_i \end{pmatrix} & 0 \le Y \le 1/2 \\ \begin{pmatrix} 1 - R_2(1 - X_i) \\ 1 - T(1 - Y_i) \end{pmatrix} & 1/2 < Y \le 1 \end{cases} \tag{19}$$

with $R_1 = 0.4$ and $R_2 = 0.6$. Strange attractors are obtained for $1 < T \le 2$ and strange repellers for $T > 2$. In this form the number of periodic orbits of period n is T^n. The number of periodic points belonging to periodic orbits of length n in the map are presented in Table 1 for four values of T, namely $T = 1.2$, 1.4, 1.8 and 2.0. N_n denotes the total number of orbits of period n in the system. The smaller the value of T, the slower the convergence of N_n to the theoretical value T^n. An n-th order approximate to the topological entropy, K_0, can be calculated from

$$K_0^{(n)} = \frac{\ln N_n}{n} . \tag{20}$$

The values of $K_0^{(n)}$ for the above values of T are listed in Table 1.

Each orbit has a unique binary label and the periodic points lie on a binary tree. The symbolic sequence of a periodic point of period n has the binary form $(a_1, a_2, \ldots, a_n)$. Numerically periodic points have been determined for orbits of period up to 32. The partition is defined by a 0 for a Y less then 0.5 and a 1 for Y greater than 0.5. Any orbit on the attractor can be represented by a pair of numbers γ and δ called the symbolic plane, where δ and γ are defined by [14]

$$\delta = 1 - \sum_{k=1}^{\infty} d_k 2^{-k} \quad \text{where} \quad d_k = \sum_{i=1}^{k} (1 - a_{-i}) \bmod 2 , \tag{21}$$
$$\gamma = \sum_{k=1}^{\infty} c_k 2^{-k} \quad \text{where} \quad c_k = \sum_{i=1}^{k} a_i \bmod 2 .$$

The symbolic plane for $T = 1.48$ is shown in Fig. 4a. Points belonging to periodic orbits of length 24 are shown. The allowed orbits are represented by blocks in the symbolic plane. In contrast, the symbolic plane for $T = 1.8$ is shown in Fig. 4b, using periodic points of length 16. With decreasing T the orbits are pruned in a systematic way. Figures 5a and 5b show the strange attractor for $T = 1.4$ and 1.8, respectively. It is apparent from these figures that, as the parameter T

Table 1. The number of periodic points belonging to periodic orbits of length n in the baker's map. The third column is the theoretical value expected from the universal grammar. The fourth column is the number of orbits obtained. The last column is the n-th order approximate of the topological entropy.

T	Period n	T^n	N_n	$K_0^{(n)}$
1.2	24	80	268	0.2329
	28	164	450	0.2182
	32	341	1 020	0.2165
	⋮	⋮	⋮	⋮
	∞	...	...	0.1823
1.48	24	12 197	12 654	0.3935
	26	26 718	27 510	0.3932
	27	39 542	38 736	0.3913
	⋮	⋮	⋮	⋮
	∞	...	...	0.3920
1.8	12	1 156	1 152	0.5874
	14	3 748	3 782	0.5884
	18	39 346	39 314	0.5877
	⋮	⋮	⋮	⋮
	∞	...	...	0.5878
2.0	13	8 192	8 192	0.6931
	14	16 384	16 384	0.6931
	15	32 768	32 768	0.6931
	⋮	⋮	⋮	⋮
	∞	...	...	0.6931

is decreased the loss of structure is related to the pruning of the periodic orbits. The stable manifold in this case lies on a pruned Cantor set.

The properties of the $f(\alpha)$ spectrum for this pruned Cantor set are investigated for three values of T, namely, $T = 1.48$, 1.8 and 2.0. Two techniques are adopted to calculate the $f(\alpha)$ spectrum. The first uses the analytic equations of Auerbach et al. [10]. However this technique has the draw back that the solution only converges for n large. The second method is to implement (9) numerically. In both cases the allowed orbits are numerically calculated.

Auerbach et al. proposed the following equation which relates the stability of the periodic orbits to the scaling exponents [10]:

$$\lambda_1^{(n)} \alpha_1 + \lambda_2^{(n)} \alpha_2 = 0 , \tag{22}$$

where α_1 and α_2 are the scaling exponents in the expanding and contracting direction, respectively, and $\lambda_1^{(n)}$ and $\lambda_2^{(n)}$ are the expanding and contracting Lyapunov exponents of period n. For uniform hyperbolic attractors the measure is absolutely continuous in the expanding direction and hence $\alpha_1 = 1$. Therefore

$$\alpha = \alpha_1 + \alpha_2 = 1 - \lambda_1^{(n)}/\lambda_2^{(n)} . \tag{23}$$

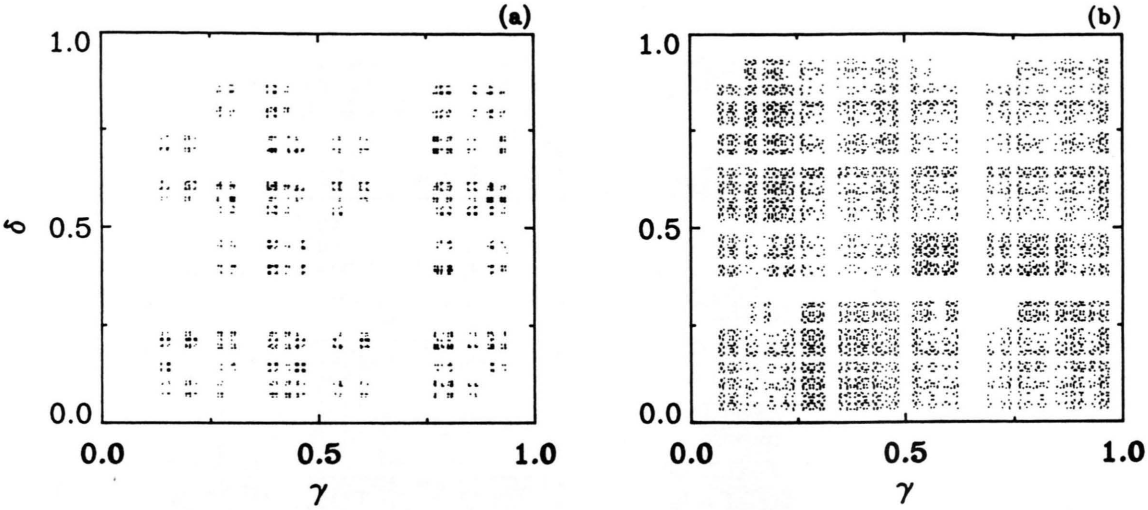

Fig. 4. The symbolic plane of the baker's map (19) for (a) $T = 1.48$ and (b) $T = 1.8$.

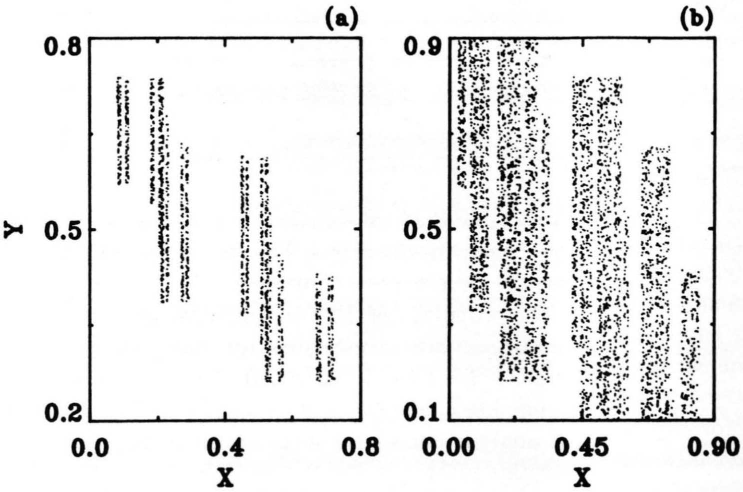

Fig. 5. The attractor of the baker's map (19): (a) $T = 1.48$ and (b) $T = 1.8$.

All that remains therefore is to locate the periodic orbits, calculate their stabilities and count how many times the value α falls into an interval of size $\Delta\alpha$. The total number is denoted by $N(\alpha)$. The value of f is calculated as follows. The typical length scale $l(\alpha)$ associated with a cycle of order n is $l(\alpha) = \exp(\lambda_2^{(n)})$. If only contributions from lower-order cycles are found, say $k < n$, then $l(\alpha) = \exp(\lambda_2^{(n)} n/k)$. Finally $f(\alpha) = \log N(\alpha)/\log l(\alpha)$, where $f(\alpha) = f(1+\alpha_2) = 1 + f_2(\alpha_2)$.

The Lyapunov exponents for (7) are

$$\lambda_1^{(n)} = n \ln(T),$$
$$\lambda_2^{(n)} = m \ln(R_1) + (n-m) \ln(R_2). \quad (24)$$

Hence, from (23) α is given by

$$\alpha = 1 - \frac{n \ln(T)}{m \ln(R_1) + (n-m) \ln(R_2)} \quad (25)$$

with $f(\alpha)$ given by

$$f(\alpha) = 1 + \frac{\ln(N_{nm})}{m \ln(R_1) + (n-m) \ln(R_2)}, \quad (26)$$

where N_{nm} is the number of orbits of period n with m 0's. For $T < 2$, N_{nm} may be zero, whereas for $T = 2$, N_{nm} is simply $\binom{n}{m}$. The convergence of the $f(\alpha)$ spectrum ((25) and (26)) can be illustrated for $T=2$, and $n=15$, with $m=0$ to n, as shown in Figure 6. It consists of 16 points represented by diamonds. The converged spectrum is shown by the continuous line. Convergence is obtained in the limit n going to infinity. Note that the convergence is good in the wings. One can use (25) and (26) to estimate the clipping once N_{nm} has been calculated numerically. However the second numerical technique we will now discuss is more accurate.

The second method converges for small values of n. Inserting the eigenvalues, (9) yields

$$\Gamma(q,\tau) = T^{-nq} \sum_{m=0}^{n} N_{nm} (R_1^m R_2^{(n-m)})^{-\tau(q)}, \quad (27)$$

where the summation is only over allowed orbits. For $T<2$ the total number of orbits, N_{nm}, is determined using the procedure discussed in Auerbach et al. [10]. For $T=1.48$ and $n=27$ the following coefficients were obtained: $N_{27,12}=306$, $N_{27,13}=19062$, $N_{27,14}=19062$, $N_{27,15}=306$; while for $0 \le m < 12$ and $15 < m \le 27$ the coefficients are zero. The symmetry of this map is reflected in the magnitude of these coefficients. After calculating N_{nm} for a chosen n, $\tau(q)$ is calculated from (27), and then the $f(\alpha)$ spectrum is obtained via the Legendre transform. The calculated $f(\alpha)$ spectrum is shown in Figure 7. The calculations converge well with similar results being obtained for orbits of period smaller than 27. For $T=1.8$, orbits of period 18 give the following coefficients: $N_{18,6}=54$, $N_{18,7}=1980$, $N_{18,8}=9720$, $N_{18,9}=15806$, $N_{18,10}=9720$, $N_{18,11}=1980$, $N_{18,12}=54$, and for $0 \le m < 6$ and $12 < m \le 18$ the coefficients are again zero. The resulting $f(\alpha)$ spectrum is also shown in Figure 7. For $T \le 1.4$ all allowed orbits contribute the same α value to the spectrum which results in a point spectrum. For $T=1.48$ and 1.8, because of the nature of the pruning, α_{max} and α_{min} correspond to a value of f greater than 1. For $T=1.8$ the orbits of period 12, 15, 18, 21, and 24 all converge to give $\alpha_{min}=1.75248$ and a corresponding $f=1.28$ and $\alpha_{max}=1.9099137$ with a corresponding $f=1.34$. Note that either technique gives good convergence in the wings of the spectrum (see Fig. 6), thus allowing an accurate determination of the clipping. Hence the wings of the $f(\alpha)$ spectrum are clipped. For $T=2$ the $f(\alpha)$ spectrum is just that of the two scale Cantor set. From (27) the Hausdorff dimension, D_0, depends indirectly on T through the coefficients N_{nm}, increasing to its maximum value of 2 when $T=2$. The experimental observation of a clipped $f(\alpha)$

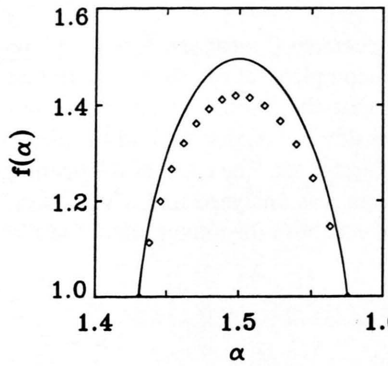

Fig. 6. The continuous line is the $f(\alpha)$ function for the baker's map (19) for $T=2.0$. The diamonds correspond to the $f(\alpha)$ function obtained from all unstable orbits of period 15. Note that the spectrum has good convergence in the wings though not at the maximum.

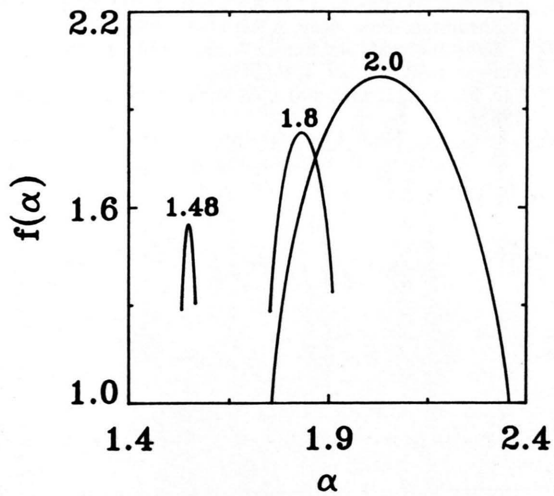

Fig. 7. $f(\alpha)$ spectra of the baker's map (19) for the parameters $T=1.48$, 1.8 and 2.0 obtained from unstable orbits of period 27, 18, and 15, respectively.

spectrum could mean that that the underlining strange attractor contains a pruned orbit structure. However there are other mechanisms which can also lead to a clipped $f(\alpha)$ spectrum, and so further careful study has to be undertaken to determine the exact origin of the clipping when working with experimental data [10]. One can not deduce the origin of the clipping purely from observation of the $f(\alpha)$ spectrum.

5. Summary

The evolution of fractal structure within the phase space of a two-dimensional hyperbolic baker's map was analyzed and quantitatively related, via its $f(\alpha)$ spectrum, to an associated Cantor set. A related baker's map with an incomplete set of orbits was studied, and it was found that the fractal structure in phase space of the map is directly related to, and characterized by, a pruned Cantor set. The effect of the pruning on the $f(\alpha)$ spectrum was analyzed and it was found that the pruning affects both the maximum of the $f(\alpha)$ spectrum and the degree of clipping of the wings of the $f(\alpha)$ spectrum.

Acknowledgements

This work was supported by EOLAS, the Irish National Agency for Science and Technology.

[1] H. Shuster, Deterministic Chaos, VCH, Weinheim 1988.
[2] V. Arnold and A. Avez, Ergodic Problems of Classical Mechanics, Benjamin, New York 1968.
[3] N. Balazs and A. Voros, Ann. Phys. (N.Y.) **190,** 1 (1989).
[4] M. Feigenbaum, J. Statistical Physics **52,** 527 (1988).
[5] M Feigenbaum, I. Procaccia, and T. Tél, Phys. Rev. **A 39,** 5359 (1989).
[6] T. Halsey, M. Jensen, L. P. Kadanoff, I. Procaccia, and B. Shraiman, Phys. Rev. **A 33,** 1141 (1986).
[7] J. Balatoni and A. Renji, Arch. Publ. Math. Inst. Hungarian Acad. Sci. **1,** 9 (1956).
[8] J. D. Farmer, E. Ott, and J. A. Yorke, Physica **7 D,** 153 (1983).
[9] I. Procaccia, Nucl. Phys. B (Proc. Suppl.) **2,** 527 (1987). – D. Auerbach, B. O'Shaughnessy, and I, Procaccia, Phys. Rev. **A 37,** 2234 (1988).
[10] D. Auerbach, P. Cvitanovic, J. P. Eckmann, G. Gunaratne, and I. Procaccia, Phys. Rev. Lett. **58,** 2387 (1987).
[11] C. Grebogi, E, Ott, and J. A. Yorke, Phys. Rev. **A 37,** 1711 (1988).
[12] J. P. Eckmann and I. Procaccia, Phys. Rev. **A 34,** 659 (1986).
[13] R. Graham and A. Hamm, Phys. Rev. Lett. **66,** 3089 (1991).
[14] P. Cvitanovic, G. Gunaratne, and I. Procaccia, Phys. Rev. **A 38,** 1503 (1988).